

## Monte Carlo simulations

Monte Carlo simulations were performed within PMOD software for a subset of time-activity curves derived from four patients presented in Figures 3, 5 and 6 in the manuscript. In each case, patient-specific input function was used that has been corrected for plasma fraction (also patient-specific) and metabolite fraction (population-based correction). The target activity concentration at each time frame was weighed by

$$w_i = \frac{1}{\sigma_i^2}, \quad \sigma_i = c\sqrt{\left(\frac{AC(t_i)}{\Delta t_i \times e^{-\lambda t_i}}\right)}, \quad (1)$$

where  $c$  is the scaling factor,  $\Delta t_i$  is the frame duration,  $AC(t_i)$  is the decay-corrected activity concentration measured at the mid-frame time  $t_i$ , and  $\lambda = \ln 2 / T_{1/2}$  is the isotope decay constant. The scale factor used was calculated from phantom experiment data, as published previously (32), taking into account the tumor size. The “true” parameters were used as starting values. After 100 fits of noisy data were performed, the distribution of the result parameters was analyzed resulting in a mean and a standard deviation value for each fitted parameter.

The mean from the 100 samples was within 1% of the “true” parameter value for all kinetic rate constants in all cases. The variance in the calculated kinetic rate constants was 1-5% for  $K_1$ , 2-15% for  $k_2$ , 2-30% for  $k_3$  and 4-50% for  $k_4$ . Larger variance for  $k_3$  and  $k_4$  was observed for the lesion shown in Figure 3A, for which “true”  $k_3$  and  $k_4$  were very low, being  $0.002 \text{ min}^{-1}$  and  $0.001 \text{ min}^{-1}$ , respectively.

32. Grkovski M, Schwartz J, Gonen M, et al. Feasibility of  $^{18}\text{F}$ -Fluoromisonidazole Kinetic Modeling in Head and Neck Cancer Using Shortened Acquisition Times. *J Nucl Med*. 2016;57:334-41.

**Supplemental Table 1.** Summary of values for metrics derived from a small region of interest (5 voxels) focused on the area of maximum  $^{18}\text{F}$ -(2S,4R)-4-Fluoroglutamine uptake on baseline PET. Mean  $\pm$  standard deviation (range).

Metric	All lesions (n=50)	All brain lesions (n=35)	Primary brain lesions (n=26)	Brain metastases (n=9)	All thoracic / abdominal lesions (n=15)
--------	-----------------------	--------------------------------	------------------------------------	------------------------------	---

SUV1	3.2±1.4 (0.9-7.1)	2.9±1.2 (0.9-5.1)	3.1±1.2 (0.9-5.1)	2.4±1.0 (1.0-4.2)	3.9±1.7 (1.5-7.1)
SUV2	2.8±1.1 (0.8-5.6)	2.7±0.9 (0.8-4.6)	2.6±0.9 (0.8-4.6)	2.8±0.7 (2.0-3.6)	3.1±1.6 (0.8-5.6)
SUV3*	2.0±0.6 (0.8-3.4)	2.0±0.6 (0.9-3.4)	2.0±0.7 (0.9-3.4)	2.2±0.5 (1.6-2.9)	2.1±0.8 (0.8-3.4)
$V_B$	0.07±0.05 (0.01-0.25)	0.06±0.05 (0.01-0.25)	0.06±0.05 (0.01-0.25)	0.07±0.04 (0.02-0.16)	0.10±0.06 (0.01-0.19)
$K_1$ (mL/min/g)	0.16±0.10 (0.02-0.38)	0.12±0.09 (0.015-0.38)	0.12±0.10 (0.02-0.38)	0.11±0.06 (0.03-0.21)	0.26±0.06 (0.18-0.38)
$k_2$ (min <sup>-1</sup> )	0.10±0.10 (0.01-0.46)	0.07±0.06 (0.01-0.24)	0.06±0.06 (0.01-0.23)	0.10±0.06 (0.04-0.24)	0.19±0.11 (0.06-0.46)
$k_3$ (min <sup>-1</sup> )	0.07±0.09 (0.00-0.42)	0.05±0.07 (0.00-0.24)	0.03±0.06 (0.00-0.22)	0.11±0.08 (0.01-0.24)	0.11±0.12 (0.00-0.42)
$k_4$ (min <sup>-1</sup> )	0.04±0.08 (0.00-0.51)	0.04±0.09 (0.00-0.51)	0.04±0.10 (0.00-0.51)	0.03±0.02 (0.01-0.09)	0.04±0.04 (0.00-0.13)
$V_T$ (mL/cm <sup>3</sup> )	4.1±1.9 (1.8-11.2)	3.9±1.8 (1.8-11.2)	3.8±1.8 (1.8-11.2)	4.5±1.4 (3.0-7.6)	4.4±2.4 (1.8-10.7)

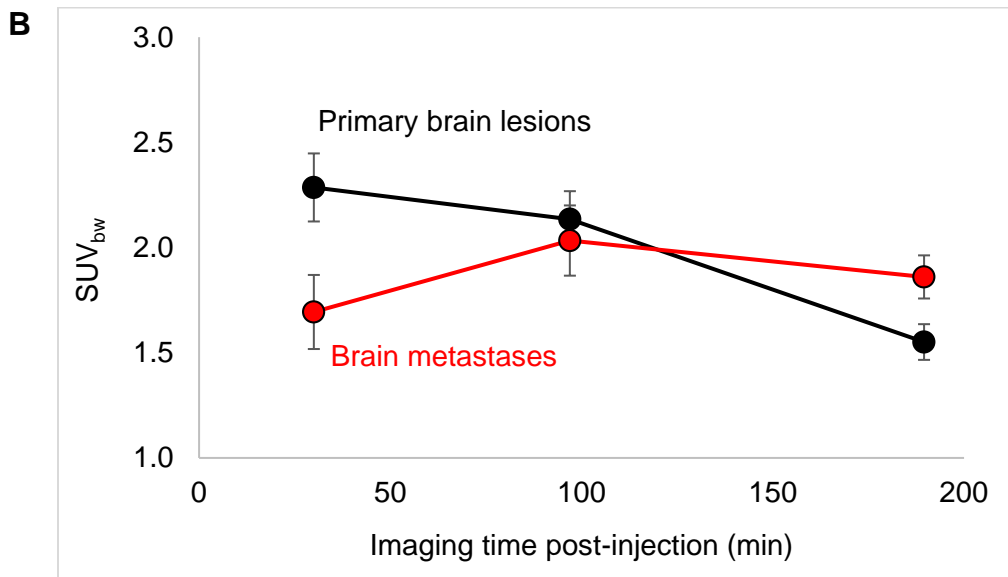
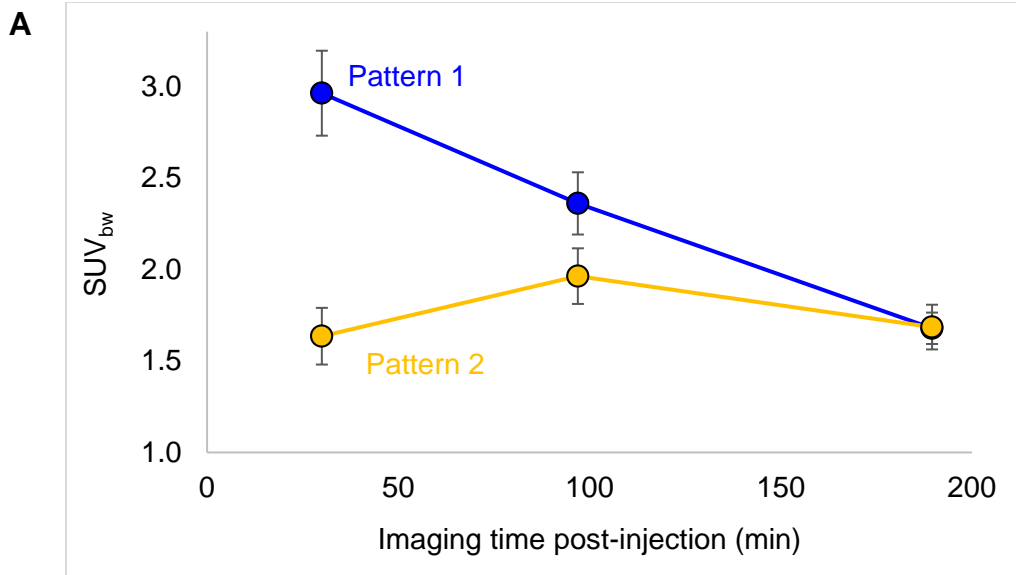
SUV1, SUV2, SUV3 - standardized uptake value, corrected by body weight, as calculated from the last 5-min frame of the 30-min dynamic acquisition, ~100-min and ~190-min PET acquisitions, respectively.  $V_T$  - Volume of distribution (Logan graphical analysis).

\*SUV3 was not measured in n=10 lesions.

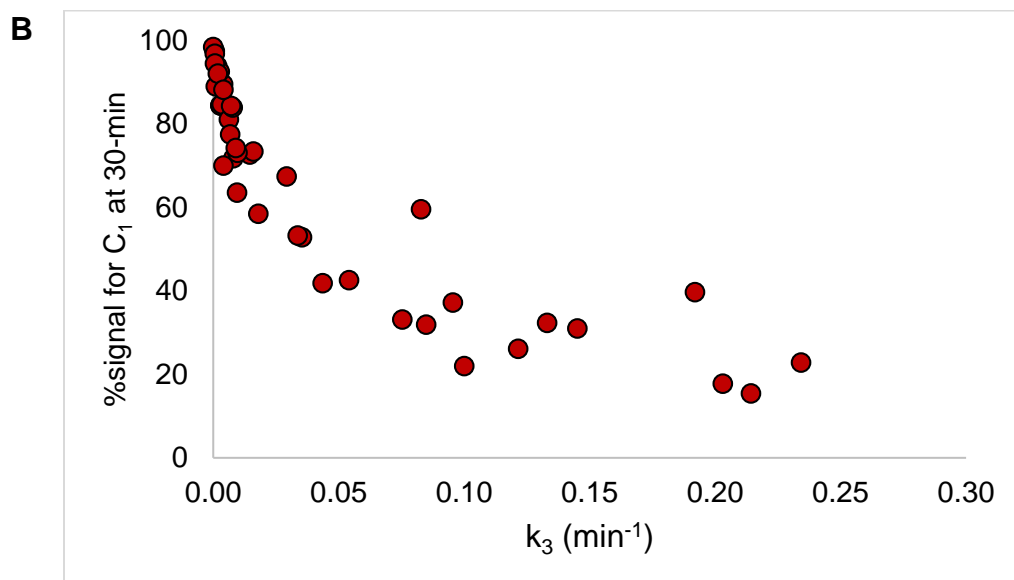
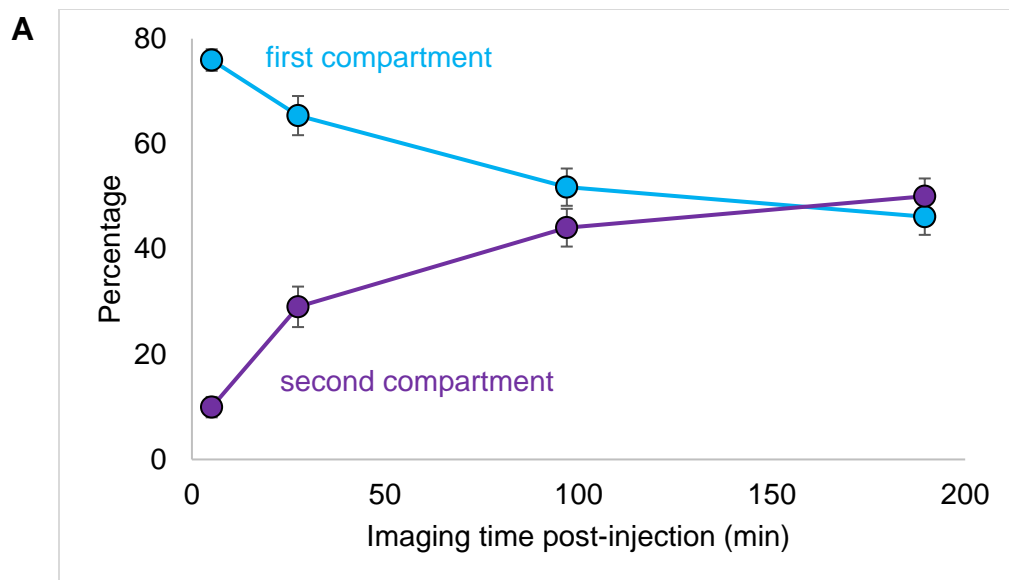
**Supplemental Table 2.** Spearman's  $\rho$  between kinetic rate constants from 2C4K model and  $V_T$  for all n=50 lesions.

	$k_2$	$k_3$	$k_4$	$V_T$
$K_1$	0.82	0.43	0.42	0.48
$k_2$		0.77	0.70	0.23
$k_3$			0.88	0.21
$k_4$				0.24

$V_T$  - Volume of distribution (Logan graphical analysis).



**Supplemental Figure 1.** (A) Continuing decrease in  $^{18}\text{F}$ -FGIn uptake after 30-min imaging time-point was observed in 29/42 evaluable lesions (69%; Pattern 1. SUV1 =  $3.0 \pm 1.3$ , SUV2 =  $2.4 \pm 0.9$  and SUV3 =  $1.7 \pm 0.5$ ), whereas a peak at ~100-min imaging time-point and a subsequent decrease was observed in the remaining 13/42 lesions (31%; Pattern 2. SUV1 =  $1.6 \pm 0.5$ , SUV2 =  $2.0 \pm 0.5$  and SUV3 =  $1.7 \pm 0.4$ ). (B) Primary brain lesions (n=26) exhibited higher  $^{18}\text{F}$ -FGIn uptake after 30-min which subsequently decreased.  $^{18}\text{F}$ -FGIn uptake pattern in brain metastases (n=9) was markedly different, exhibiting a slower initial accumulation and a more sustained peak due to higher rate of glutaminolysis. Mean  $\pm$  Standard Error.



**Supplemental Figure 2.** (A) Percentage contributions to total PET signal from first (C<sub>1</sub>) and second (C<sub>2</sub>) compartment as a function of imaging time post-injection averaged over all n=50 lesions. Mean ± Standard Error. (B) Scatterplot of mean intratumor k<sub>3</sub> as percentage signal from 1<sup>st</sup> compartment, as measured at 30-min post-injection. Spearman's  $\rho = -0.97$ .